Tunnelling and Underground Space Technology 33 (2013) 34–45

Contents lists available at SciVerse ScienceDirect

Tunnelling and Underground Space Technology

journal homepage: www.elsevier.com/locate/tust

Influence of the fault zone in shallow tunneling: A case study of Izmir Metro Tunnel

Mete Kun *, Turgay Onargan

Department of Mining Engineering, Dokuz Eylül University, Tınaztepe Campus, Buca, 35160 İzmir, Turkey

ARTICLE INFO

Article history:
Received 16 February 2012
Received in revised form 26 June 2012
Accepted 30 June 2012
Available online 16 November 2012

Keywords:
Shallow tunnel
Fault zone
Weak rock
New Austrian Tunneling Method

ABSTRACT

Today, there is a great need for larger underground spaces for various purposes and hence, construction of new metro tunnels has become a necessity to meet the demand in urban life in spite of certain ground related difficulties such as fault zones, altered and fractured rock mass and ground water. This study has aimed at investigating the risky areas around a shallow metro tunnel in weak, faulted rocks and determining the effects of tunnel behavior on the structures on ground surface. Therefore, an attempt has been made to determine the risky areas on the line of the tunnel by field observations, laboratory work and computer modeling. Later, the data obtained from computer models have been compared to which obtained from in situ measurements. The results from modeling and in situ measurements were interpreted considering the current status of superstructure and the differences between pre- and post-excavation states in the ground. Finally the data obtained from the modeling analysis and measurements provided the necessity of strengthening the already used support system for the safety of the buildings on surface. Shortening the application ranges of the rock bolts, use of face nails with application of umbrella arc and jetgrout methods are among the precautions to be taken.

1. Introduction

Growing populations, increasing oil prices and new developments in urban areas have increased the demand for rapid underground metro railway networks for mass transportation. Metro tunnels are usually opened at shallow depth in weak rock or soft soil conditions. Hence, faulting and frequent fractures in rock, low bearing capacities of soil, large deformations and underground water dynamics can induce difficulties during the construction of metro tunnels.

Basic parameters studied by Whittaker and Frith (1990), which influence the stability of tunnels in soft soil and weak rocks can be listed as the strength of intact rock and the rock mass and other geomechanical properties, excavation induced stresses, method of excavation, applied support systems and dynamics of underground water. Therefore, detailed geological and geotechnical investigations must be conducted along the route of tunnel in order to propose the most appropriate excavation and support method and to minimize the possible risks due to tunneling activities (excavation, support and drainage, etc.). Excavation process must be initiated and sustained under control, following evaluations and verifications of the computer modeling of proposed methods. Tunnel excavation must be maintained under control by continuous deformation measurements, exploratory boreholes and the experiences gained from previous tunneling works in the region (Onargan et al., 2009).

Bell (1994) has defined an order for tunnel advancing and processing to minimize the risks during the opening of tunnels. In his definition, a structure which takes into account the field investigations, experiences and estimations, results of the models used, regular in situ measurements has been formed to maintain controllable advancement of the tunnel. Certain techniques relying on analytical, empirical or numerical solutions can be found in the literature. Each technique may possess certain advantages and disadvantages. Hence, the use of at least two of them simultaneously may yield more reliable results and enable comparisons of the solutions for justification (Ulusay, 2001).

Also, the geology forms the basis for all rock engineering works, such as field investigations and the following rock engineering evaluations. Wrong geological interpretation will affect all engineering analyses and calculations based on the geological model. An important feature in geology is the occurrence of possible faults and weakness zones, as well as rocks and/or minerals with special properties and/or behavior (Stille and Palmstrom, 2008).

In this study, the fault zone and surroundings, defined as risky area, on the route of the 2nd Stage of Izmir Metro Tunnel Project were investigated in detail based on the principles of New Austrian Tunneling Method (NATM) at a shallow depth (18–25 m). The data in hand, results of laboratory tests (conducted in compliance with ISRM (1981)) and the results of numerical modeling were compared with in situ measurement values obtained during the excavation of tunnel in order to examine the potential risks in

* Corresponding author. Tel.: +90 232 412 75 40; fax: +90 232 453 08 68.
E-mail address: mete.kun@deu.edu.tr (M. Kun).

0886-7798/$ - see front matter © 2012 Elsevier Ltd. All rights reserved.
http://dx.doi.org/10.1016/j.tust.2012.06.016

tunnel itself and on surface structures, due to the existence of fault zone.

2. Location and geological structure of study area

Study was conducted in the frame of 5640 m long Izmir 2nd Stage Metro Tunnel Project in the south of Izmir Province located in western Turkey (Fig. 1). Geological units crossing the tunnel route can be listed as: Vulcanites, alluviums, sandstones, claystone, pebblestones (Altindag formation), clayey limestone sequence and flysch. These lithological units are overlaid by an artificial filling material on the surface. Vulcanites of Miocene age, extensively spreaded on the route of tunnel, have been formed of andesites of gray colored medium size grains, low-to-medium alteration and medium-to-dense spaced, clay filled joints.

The agglomerate contains andesite pebbles and blocks of 0.5–30 cm in size and has reddish brown color, moderately altered, open and planar joints with clay-filling and low-to-medium strength. Miocene aged Altindag formation consists of sequences of claystone, siltstone, sandstone and conglomerate. This formation is covered with alluvium and artificial fill. It outcrops the Bornova flysch beneath it. The units of Altindag formation are medium-to-high altered, medium-to-densely jointed and possess low-to-medium strength. Also, they display vertical–lateral transition with local vulcanites owing to their common geological ages. Study area and its surrounding geology are shown in Fig. 2.

2.1. Tectonics and local geology of near fault zone

When tectonics of the region along the tunnel route was investigated one can notice the existence of active faults in Izmir and its surroundings. Active faults in Izmir and nearby have been mapped by Saroglu et al. (1992). Later, Barka et al. (1996) and Emre and Barka (2000) have reported that number of active faults in this region was more than anticipated.

Field studies conducted on the tunnel route unveiled that tunneling operations can be affected due in part to Izmir Fault (Emre and Barka, 2000). Data on the characteristics of this fault are limited due to the intense urban settlement in the area (Fig. 3). However, geomorphological features of E–W oriented Izmir Fault were found to resemble that of normal faults (MTA, 2005).

Fault zone which is expected to influence the 5460 m long metro tunnel to be excavated was investigated in detail by geological field studies and evaluations in the area. Therefore, near Goztepe Station located at distances of 2 + 447.75 – 2 + 655.48 km, detailed information of fault zone and lithological units was collected by means of five boreholes (S15, S16, S16-A, S17, S18). Accordingly, dominating rock units in and the near fault zone were determined to be Altindag formation, andesite and alluvium (Fig. 4).

Altindag formation consists of claystone, siltstone and conglomerate units. Claystone has poor strength and displays light green and gray; light yellow to brown color, medium to well alteration, medium to dense jointing properties. It demonstrates fair plasticity owing to the possession of loose filling and high saturation degree.

Siltstone has poor to medium strength and displays green, yellow to brown color, medium to well alteration. It is well compacted and cemented with clay and carbonates. Joint surfaces are smooth and unfilled or clay filled.

Sandstone demonstrates poor to medium strength and has light gray, light yellow to brown color, medium to high alteration. It is cemented with carbonates and length of the pebbles varies between 0.4 and 4 cm. Joint surfaces are rough and partially filled with clay of 0.5 cm thickness.

Conglomerate is of poor to medium strength and has light gray to gray color and high alteration degree. It is cemented with clay, silt, sand and carbonates and the diameters of the pebbles vary between 0.5 and 5 cm. Joint surfaces are usually unfilled.

2.2. Hydrogeology

Geological units present on tunnel route depict hydro geological properties owing to their unique characteristics. Underground water is let to circulate depending on the granular structure of soil units, lithological properties and characteristics of joint sets of the rock mass. Clay unit in alluvium and impervious sand and pebble levels contain underground water. The tuff unit within vulcanites, lightly altered andesite and agglomerate units is impervious; however, well altered andesite and agglomerate enable the flow of underground water along the fractures. Sandstone and conglomerate ranges of Altindag formation allow the flow of underground water whereas the claystone unit is impervious.

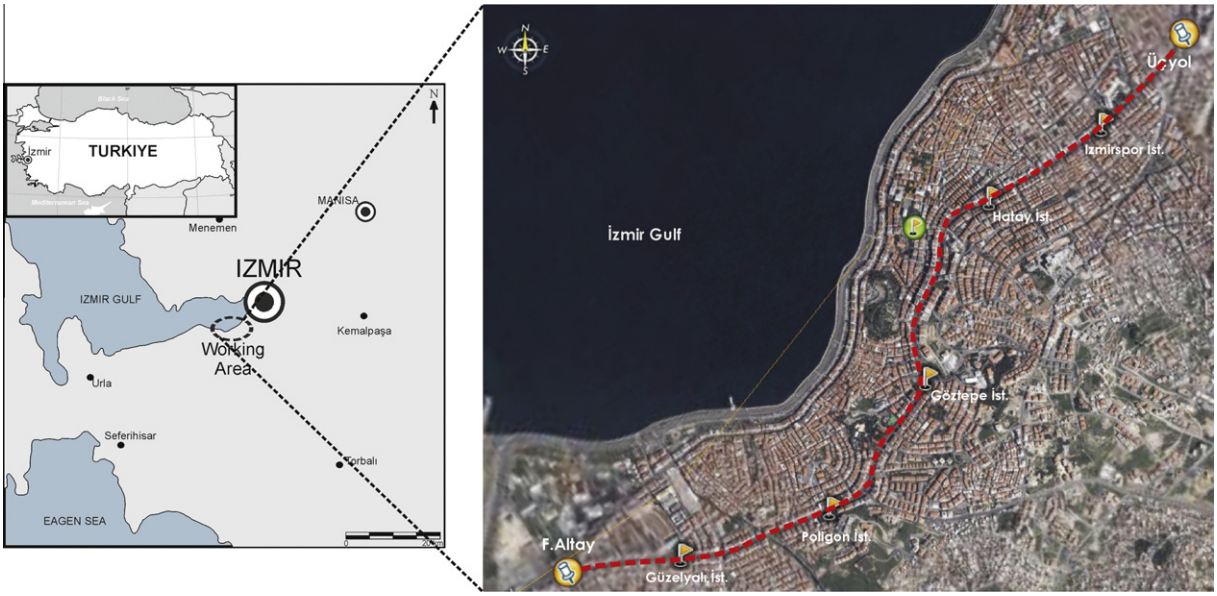

Fig. 1. Location map of the study area.

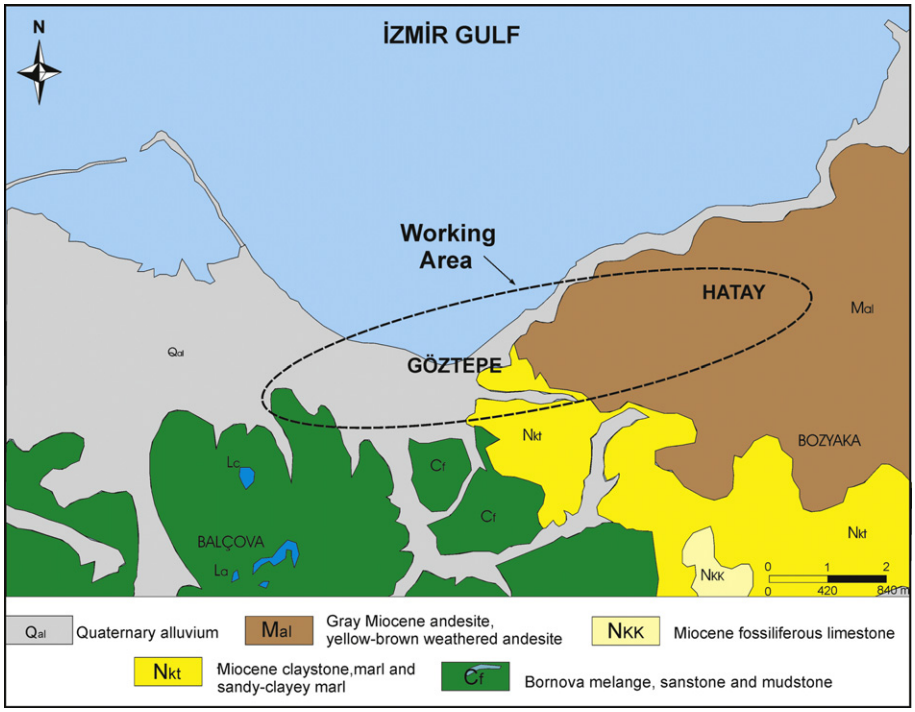

Fig. 2. General geology of the vicinity of study area (Kun, 2010 rearranged).

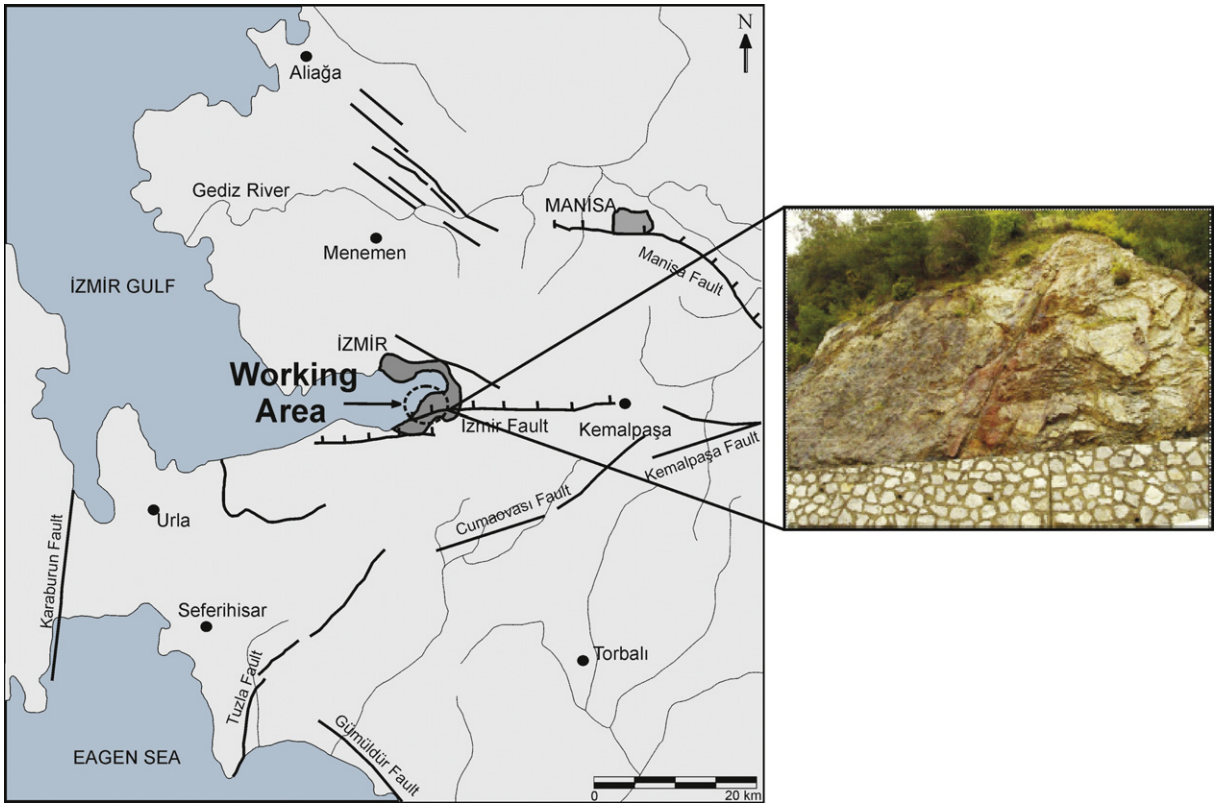

Fig. 3. Fault map indicating the active faults on tunnel route and surroundings in the study area (MTA Report, 2005 rearranged).

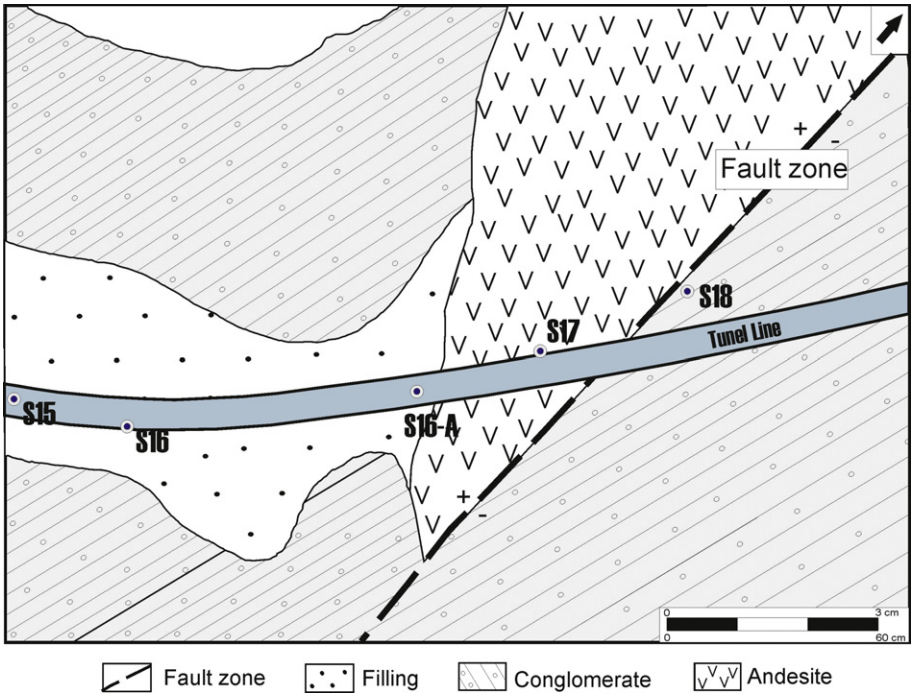

Fig. 4. Borehole locations near fault zone (Geotechnical evaluation report of Izmir light rail system 2nd Stage 2nd Part.)

3. Engineering properties of the rock mass near fault zone and applied tunneling methods

Knowledge of engineering properties of rocks in and near the fault zone bears a great significance from the stand point of predicting rock mass behavior, determining excavation and support requirements, measures to be taken and computer modeling studies (Kun, 2010). Therefore, laboratory tests were conducted on the rock samples taken from the boreholes near the fault zone and face of the excavation. Rock units logged in the boreholes drilled near the fault zone can be listed from top to down as: fill material, alluvium and Altindag formation (Miocene aged sedimentary rocks). Engineering properties of these units are described as follows. In the excavation zone, an artificial coating layer of 2–3 m thickness lies on the top with a unit weight of 13 N/m^3, a cohesion of 0.065 MPa and an internal friction angle of 17°. Beneath, alluvium layer of 5 m thickness exists. Alluvium consists of separated grains with various dimensions and displays no cementation between the grains.

Average Rock Quality Designation (RQD) values for the units of Altindag formation were found to be 0–40% at the excavation level, according to Deere and Deere (1988). Formation was also classified to Barton's *Q* and Bieniawski's RMR rock classification systems. *Q* and RMR values were determined to be *Q* = 0.12–0.70 as very weak rock and RMR = 22–35 as weak rock (Barton and Grimstad, 1994; Bieniawski, 1989).

The values of Core Recovery (CR), RQD and rock quality descriptions for Altindag formation are displayed in Table 1. In Table 2, point load test (PLT) index values are illustrated for the same rock formation. On tunnel route, beneath the alluvium unit claystone–siltstone–sandstone–conglomerate units were intersected at various thicknesses in the borehole S-15. These rock units can also be seen on the excavation face at distances of 2 + 400 – 2 + 450 km of the tunnel route (Fig. 5).

In Table 3, certain engineering properties of the rocks near the fault zone, such as dry unit weight (DUW), uniaxial compressive strength (UCS), *Q* and RMR values are demonstrated.

In Table 4, the results of the laboratory tests on the samples taken from the excavation face are shown. These values were used as data in numerical modeling of tunnel opening through the fault zone.

Excavations in the main route tunnel (type 1) and station tunnel (type 2) make up more than 90% of the project. In Figs. 6 and 7, cross-sections, support members and excavation details are shown for both tunnel types respectively. Type 1 tunnel is of 6.45 m height and cross-sectional area of 64 m^2 whereas type 2 tunnel is of 7.73 m height and cross sectional area of 113 m^2.

4. Fault zone in tunnel area

The fault zone which was investigated by geological and borehole studies on tunnel route, appears to divide andesite unit from Altindag formation. Stochastic status prior to the tunneling and post-tunneling factual status are demonstrated by longitudinal sections. Fig. 8 shows the geological structure of the area, possible location of the fault and approximate location where the tunnel intersects the fault zone.

Table 1
CR, RQD and rock quality definitions for Altindag formation.

Borehole no.	Lithology	CR	RQD	Rock quality
S15	Conglomerate–marl–sandstone	10–100	0.0–40	Very poor–poor
S16	Sandstone–claystone	60–78	0.4–10	Very poor

CR: Core Recovery values; RQD: Rock Quality Designation.

Table 2
PLT index (Is) values for Altindag formation.

Borehole no.	Sample	Depth (m)	Sample type	Alteration degree	Is (MPa)
S15	2	29.50	Claystone	High	3.06
S16	3	25.40	Sandstone	Slightly	4.62

PLT: point load test.

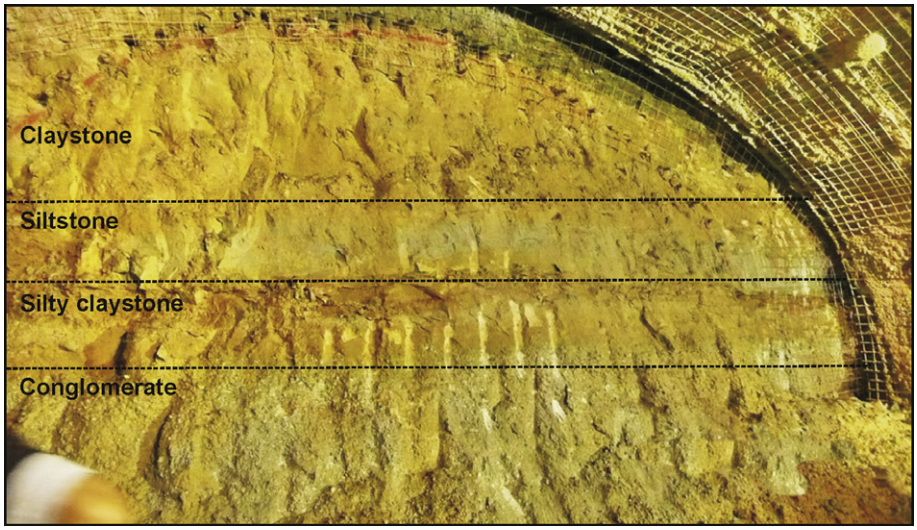

Fig. 5. Various rock units which form the Altindag formation seen on the excavation face.

Table 3
Engineering properties of Altindag formation for the fault zone.

Sample type	Alteration degree	DUW (g/cm^3)	UCS (kg/cm^2)	Q	RMR
Siltstone	High	2.32	230.1	0.002	2 – Very poor
Sandstone	Low–high	2.19	207.8	0.021	5 – Very poor
Claystone	High	2.06	160.8	0.002	2 – Very poor

DUW: dry unit weight; UCS: uniaxal compressive strength.

Table 4
Engineering properties of the formations in and near the fault zone.

Formation	Andesite	Altindag formation (sandstone, claystone, conglomerate)
Young's modulus (MPa)	64.000	700
Poisson's ratio	0.30	0.35
Internal friction angle (°)	42	18
Cohesion (MPa)	0.30	0.18

Geological explorations carried out via boreholes drilled on tunnel route indicate that Goztepe Station, which is only 80 m from the fault zone is within the sequence of Miocene aged sandstone–claystone and conglomerate units. However, details of the fault zone, which was totally covered with dense superstructuring, could only be seen on the excavation face during the construction of tunnel. Situation of the fault oriented in NS on the surface is given in Fig. 9. This normal fault which can also be seen on the intersection of type 2 and type 1 tunnels is oriented 65° in NE–SW, dipping SE as depicted in Fig. 10. As seen in Fig. 8, there is no sign of faulting traces during the tunnel planning study in both bore holes. Fault traces were observed after the tunnel was driven into the formations (Fig. 9). Thus, it was not possible to anticipate the correct position of the fault using the borehole core logging during tunnel design studies.

4.1. Computer modeling in fault zone

In order to examine the potential influence of tunneling on superstructure and tunnel cross section a 2D numerical modeling study was carried out in the fault zone which intercepts the tunnel route, using Phase 2 (Rockscience, 2006a,b) based on the parameters of "Strength Factor" and "Total Displacement" as frequently cited in the literature. Effects of tunneling on the buildings and other surface structures built in the influence zone of the tunnel were numerically investigated and the results were compared with which obtained by in situ measurements and hence, the reliability of the results of computer model was tested for the true behavior of the tunnel upon completion.

In computer modeling, the rock mass around the tunnel was simulated by finite, whereas rock mass in the immediate and far field of excavation face was simulated by boundary elements. Therefore, the rock mass displaying non-linear (elasto-plastic) and heterogenous behavior might be evaluated together with the discontinuity planes.

Data required for the application computer modeling may be gathered in two different groups, such as the properties of rock formation and support parameters. Properties of rock formation can be listed as unit weight, modulus of elasticity, Poisson's ratio, internal friction and cohesion of the soil, which were determined on the samples taken from the rocks near the fault zone as shown in Tables 2 and 3. Support parameters required to design the fault-tunnel intersection for type 1 and type 2 tunnel cross sections are given in Table 5. In computer analyses, pressure applied by the buildings on tunnel route was incorporated by assuming surcharge for a 6-story building to be 1.50 ton/m^2.

Computer models were assessed by taking the values in Table 5 into consideration for type 1 and type 2 tunnel geometries and

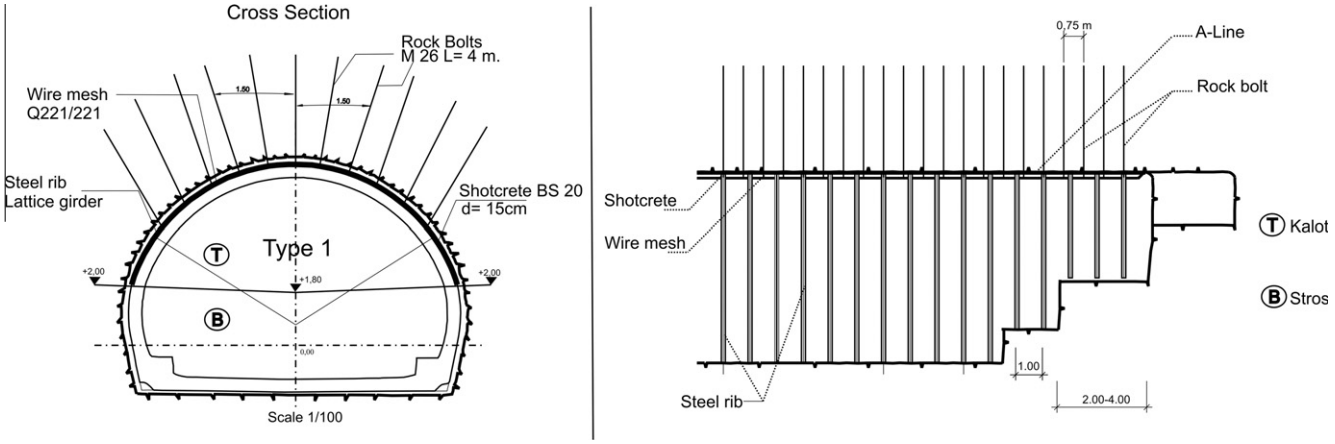

Fig. 6. Type 1 tunnel – main route.

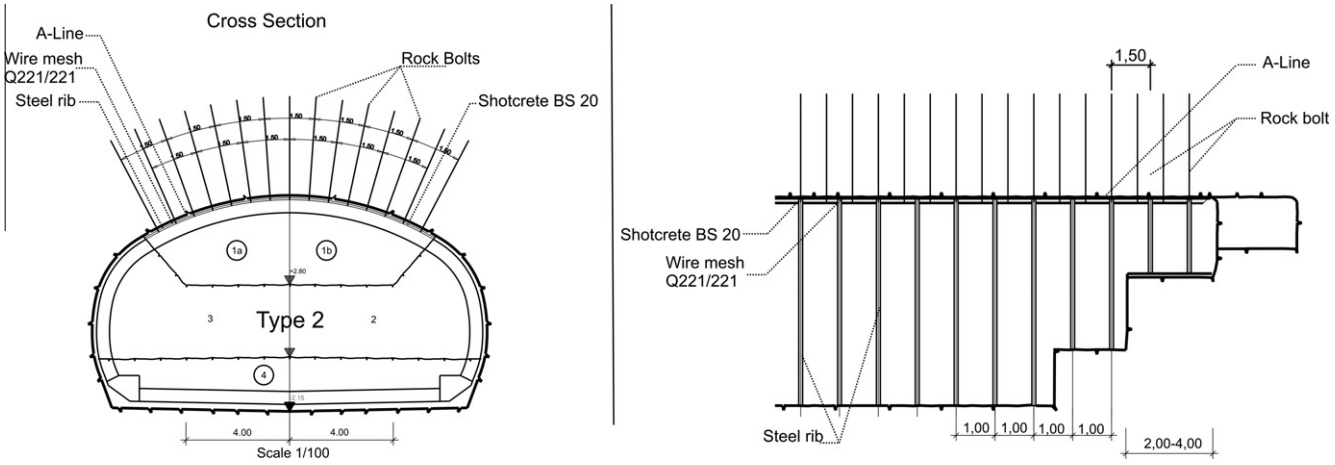

Fig. 7. Type 2 tunnel – station.

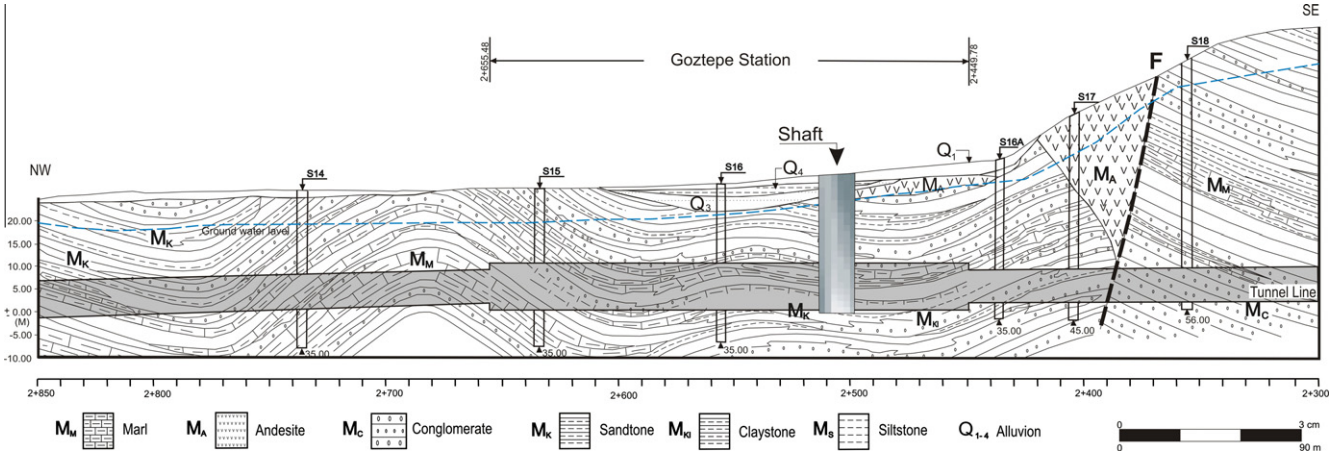

Fig. 8. Anticipated state of the fault prior to the excavation.

support elements as given in Figs. 6 and 7. The model proposed is displayed in Fig. 11 and results of the analyses obtained for the tunnel and risky areas above the tunnel are shown in Fig. 12.

In modeling, post-excavation displacements at the crown of the tunnel were evaluated for both tunnel cross sections. Average displacements at the crown of type 1 and type 2 tunnels were found to be 18–19 mm and 11.5–12 mm respectively. Similarly, surface subsidence values above the tunnel-fault zone intersection were calculated as 18 mm and 13 mm for type 1 and type 2 tunnel geometries respectively. Average deformations on the walls of both tunnel types were determined to be 3–7 mm after the installation of support.

Based on the analyses performed in unsupported tunnels horizontal to vertical stress ratio (K) was determined to vary between

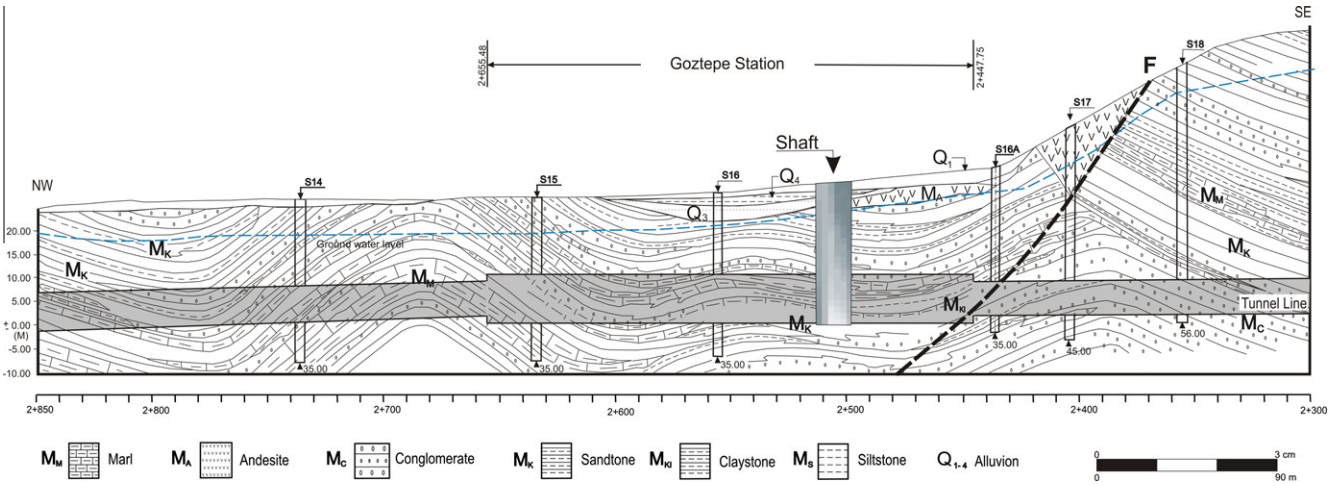

Fig. 9. State of the fault during excavation.

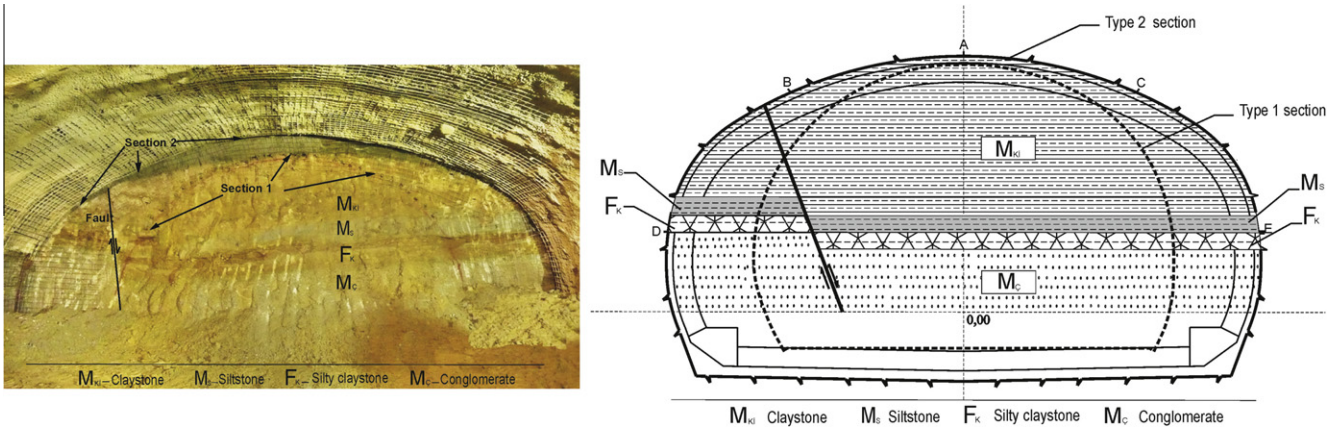

Fig. 10. Fault zone at tunnel face (type 2 to type 1 intersection).

Table 5
Tunnel excavation and support parameters.

Parameters	Value
Height	Type 1 – 6.45 m Type 2 – 7.73 m
Excavation area	Type 1 – 64 m^2 Type 2–113 m^2
Support parameters (NPI 120)	
Material behavior	Elastic
Young's modulus	210.000 MPa
Poisson's ratio	0.2
Thickness	0.00143 m
Shotcrete parameters	
Material behavior	Elastic
Young's modulus	7.000 MPa
Poisson's ratio	0.25
Thickness	0.15 m
Rock bolt parameters	
Length	4 m
Distance between rock bolts	1 m

6.89 and 10.5, which obviously can be a strong precursor for the tensile and shear failures on the walls of the tunnels. Nevertheless, considerable deformations around the tunnels and hence, on surface structures above the tunnel-fault intersection (called as 'risky') area are expected to take place, as shown in Figs. 12 and 17.

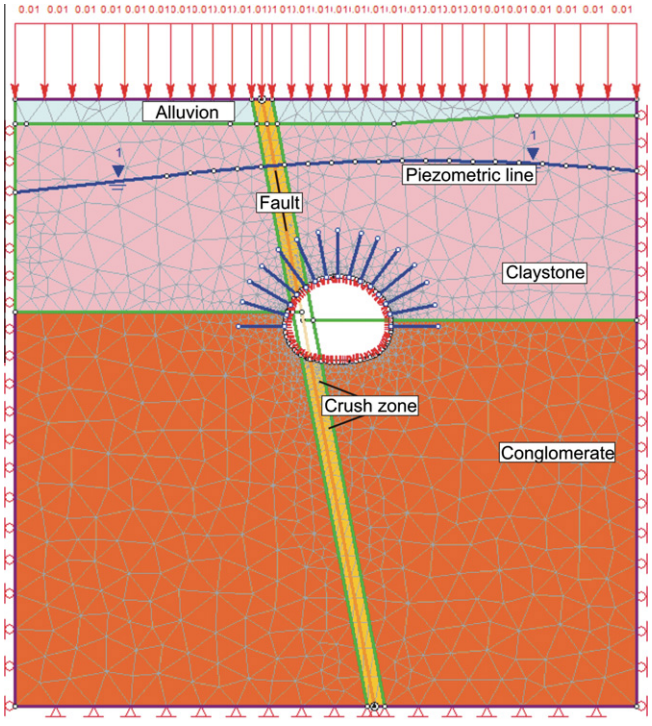

Fig. 11. The model proposed at fault zone contact.

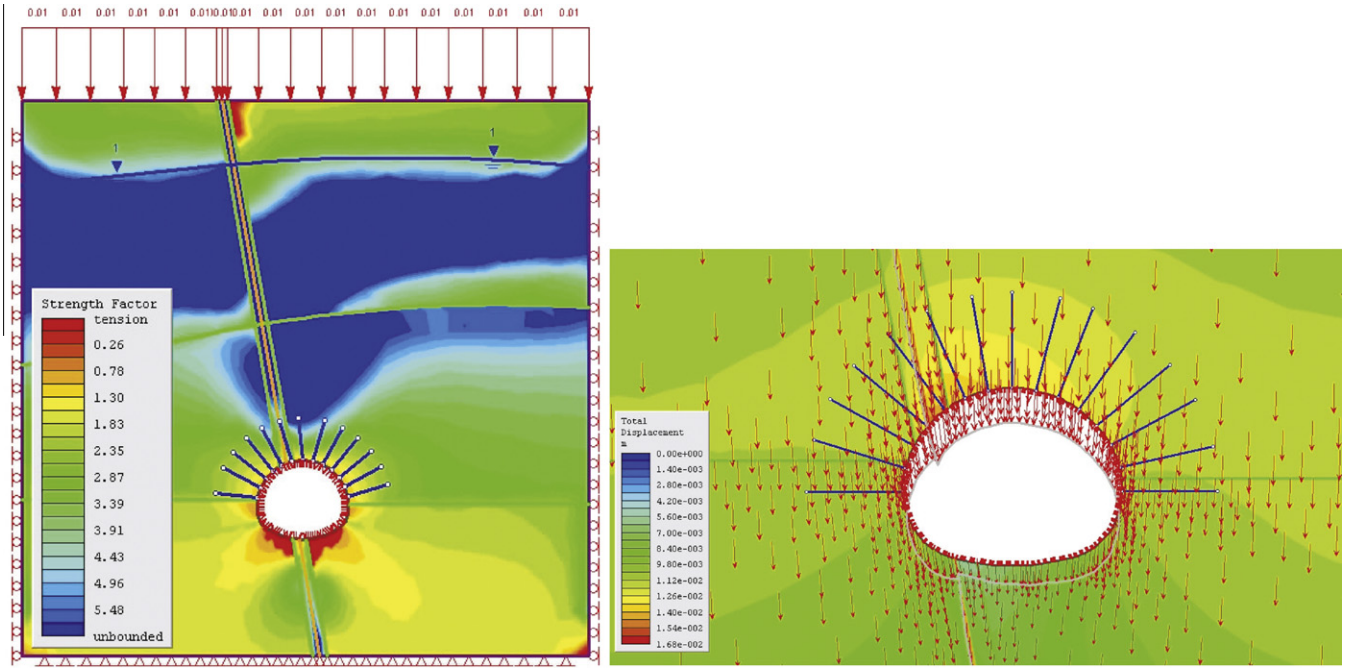

Fig. 12. Total convergence around the tunnel, on the ground surface and potentially risky areas around the tunnel.

4.2. Rock–support interaction analysis

Analyses of rock–support interaction and deformations were performed using RocSupport software (rockscience) in order to evaluate rock failure and support stability depending on the advance of excavation. Approximation based methods for determining the extent of plastic zone around a circular excavation and ground-reaction curves were used based on the consideration that

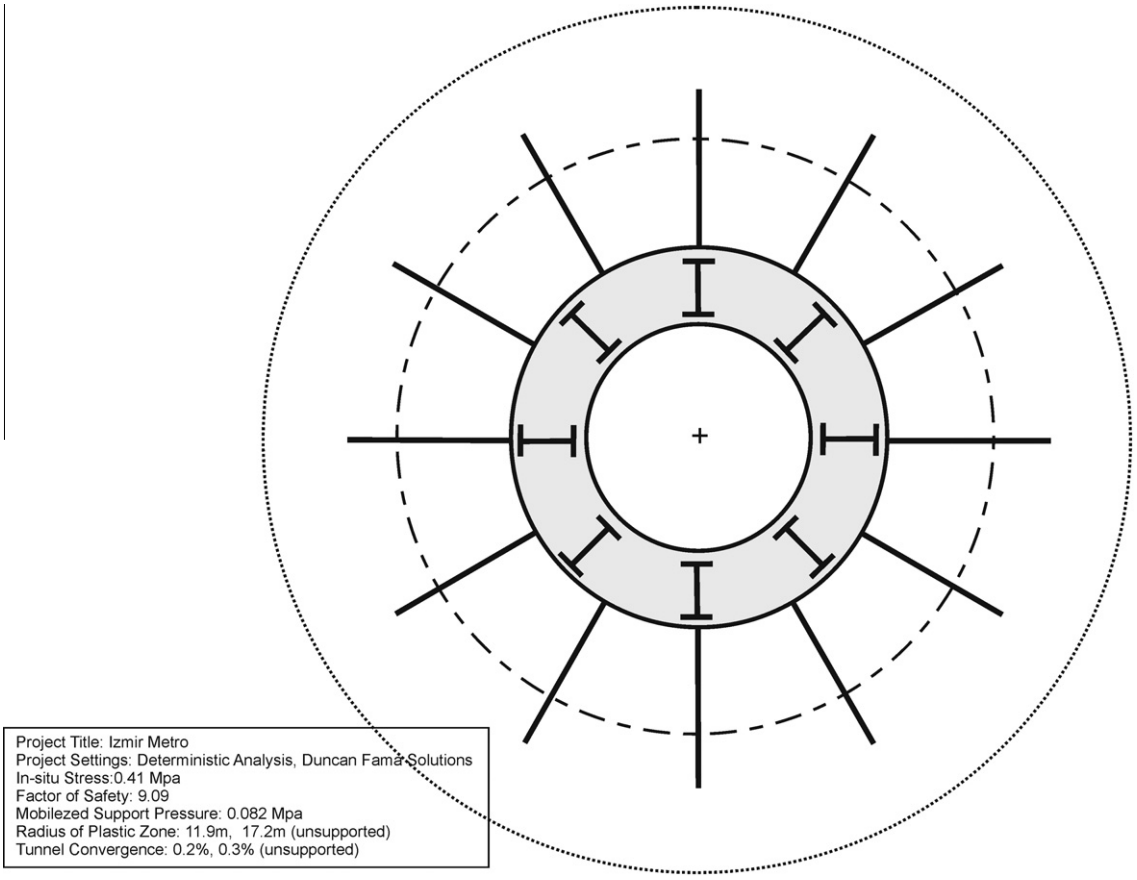

Fig. 13. Rock-support interaction analysis.

Table 6
Rock–support interaction results.

Properties	Values	
	Unsupported status	Supported status
Plastic zone radius (m)	17.2	11.9
Wall displacement amount (mm)	26	11
Tunnel convergence	0.3% (30 mm)	0.2% (20 mm)

isostatic stress conditions for soft and poor rocks and hydrostatic stress conditions for the rocks bearing ground water would be assumed in the analyses of the fault zone at the distance 2 + 400 – 2 + 500 km.

Tunnels were designed based on the safety factor of at least 9, taking into account the facts that the life span of the tunnel would be more than 100 years and metro tunnels, which usually have unique structuring must be constructed considering the worst case

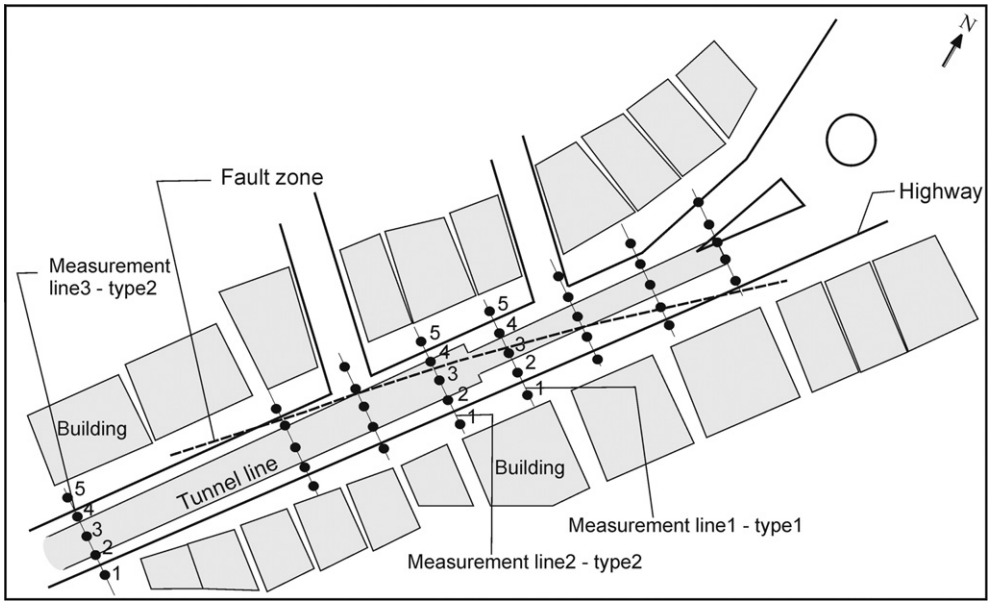

Fig. 14. Subsidence measurement lines on tunnel route at the transition of fault zone.

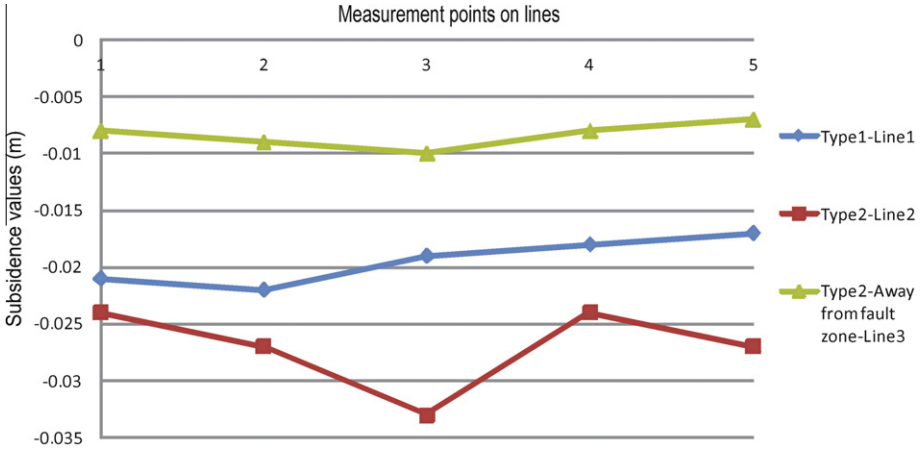

Fig. 15. Ground subsidence values for type 1 and type 2 tunnel geometries in and near the fault zone.

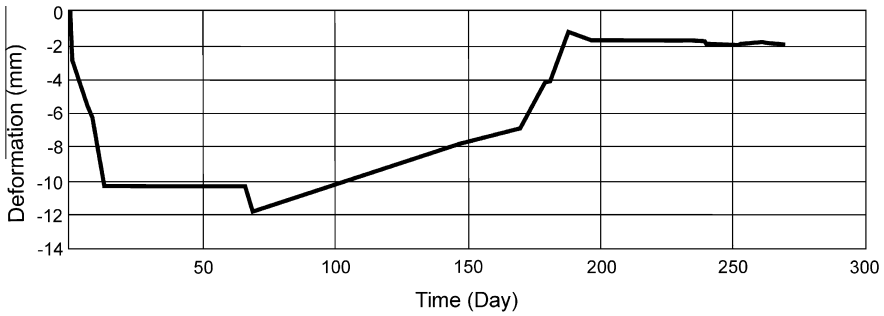

Fig. 16. Time dependent tunnel wall convergence values.

scenarios of applied loads and failure conditions (Fig. 13). The data obtained from the analyses for type 2 tunnel cross section are given in Table 6. All the data collected during this study were evaluated in Section 5.

4.3. Measuring system and the results

Deformations occurred on ground surface in and near fault zone were determined by regularly reading the subsidence rates on subsidence monitoring bolts installed at certain distances along the tunnel route (Fig. 14). Subsidence values were read and used in determining the effects of tunnel excavation on the buildings on ground surface. The maximum subsidence value was recorded when the tunnel face was just below the measuring location. Subsidence values were to be read on five monitoring bolts per measurement line since the tunnel route was directly under the state highway. The values recorded from two different measurement lines (lines 1 and 2 in Fig. 14) for type 1 and type 2 tunnel cross sections are given in Tables 7 and 8. Ground deformation values read on the monitoring bolts placed on measurement line 3, which is 50 m away from the fault zone, are displayed in Table 9.

Subsidence values measured at in situ monitoring stations along the measurement lines in the fault zone and away from the fault zone are given comparatively in Fig. 15, in which it can be seen that subsidence values recorded at the stations within the fault influence zone are considerably higher (~33 mm – *it must be less than* 10 mm *according to limits*) than that recorded at the stations away from the fault zone (~8 mm). Time dependent deformations on the walls of the tunnel were also measured and displayed in Fig. 16, in which it can be noted that tunnel deformations reached a maximum value of 12 mm and then reduced to 2 mm after 200 days, along a total testing duration of 260 days. As seen in figure, tunnel deformations were reduced from 12 mm to 2 mm after the advanced tunnel face. Deformation of 12 mm was observed when the fault zone location was very close to the tunnel face working. On the other hand, after the tunnel face move away from the fault zone, observed wall deformation value was reduced up to 2 mm at the end of 260 days in the tunnel.

5. Results and discussion

5.1. Results

In this study, influence of deformations and subsidences in and around a metro tunnel constructed as part of the 2nd Stage of Izmir Metro Project, in two different tunnel cross sections and in weak and faulted rock mass was investigated on the surface structures along the tunnel route. Therefore, detailed geological explorations and based on which computer modeling studies were conducted prior to the excavation. Following the excavation, the results obtained from computer models were compared with the deformations measured in the tunnel and on the ground surface and accordingly, it was suggested that excavation and support systems in original project be re-evaluated.

Subsidence calculations above tunnel-fault transition location were implemented by the analyses of 2D computer models. Besides, it was attempted to predict the tunnel behavior in the fault zone by rock–support interaction analyses prior to the excavation. After the excavation, the values of in situ deformation measurements in the tunnel and on the ground were compared with the results obtained from computer models.

Computer models yielded following results at tunnel-fault transition:

- subsidence of 18 mm for type 1 tunnel geometry,
- subsidence of 13 mm for type 2 tunnel geometry,
- convergence of 19 mm at the crown for type 1 tunnel geometry,
- convergence of 12 mm at the crown for type 2 tunnel geometry,
- convergence of 3–7 mm at the walls for both type 1 and type 2 tunnel geometries.

Post-excavation in situ displacements were measured at tunnel-fault transition as follows:

- subsidence of 19 mm for type 1 tunnel geometry,
- subsidence of 27 mm for type 2 tunnel geometry,

Table 7
Ground subsidence values read for the cross section of type 1 tunnel (measurement line 1).

Point no.	First reading (m)	Last reading (m)	Value (m)
1.1	28.083	28.062	−0.021
1.2	27.953	27.931	−0.022
1.3	28.032	28.013	−0.019
1.4	27.949	27.931	−0.018
1.5	28.166	28.146	−0.017
Mean	−0.019		

Table 8
Ground subsidence values read for the cross-section of type 2 tunnel (measurement line 2).

Point no.	First reading (m)	Last reading (m)	Value (m)
2.1	28.677	28.653	−0.024
2.2	28.463	28.436	−0.027
2.3	28.511	28.478	−0.033
2.4	28.445	28.421	−0.024
2.5	28.631	28.604	−0.027
Mean	−0.027		

Table 9
Ground subsidence values read for the cross-section of type 2 tunnel (line 3), outside the fault zone (away from fault zone).

Point no.	First reading (m)	Last reading (m)	Value (m)
3.1	28.478	28.470	−0.008
3.2	28.512	28.503	−0.009
3.3	28.555	28.545	−0.010
3.4	28.453	28.445	−0.008
3.5	28.587	28.580	−0.007
Mean	−0.008		

Table 10
Estimated and observed values for the convergences, deformations and subsidences during the tunnel driven in the formations.

	Estimated values (pre-excavation)	Measurement values (post-excavation)
For type 1 tunnel geometry		
Convergence (mm)	19	10–11
Subsidence (mm)	18	19
Average deformations on walls (mm)	3–7	12
For type 2 tunnel geometry		
Convergence (mm)	12	10–11
Subsidence (mm)	13	27
Average deformations on walls (mm)	3–7	12

- convergence of 10–11 mm at the crown for both type 1 and type 2 tunnel geometries,
- convergence of 12 mm (see Fig. 16) at the walls for both type 1 and type 2 tunnel geometries.

As shown in 'measurement line 3' in Fig. 14, a subsidence of 8 mm was measured at a distance of 50 m away from the fault zone.

The steps of excavation and timing of erection of support in shallow metro tunnels opened in a weak ground must be planned by careful evaluations of geological and geotechnical data available and taking into consideration the damage which may occur on surface structures above the tunnel route. Otherwise, it is very likely that significant settlements and damage may occur in the buildings and other structures during the installation of support, if not placed timely. Maximum surface settlement value is predicted as 10 mm, which, as can be found in the literature for similar ground conditions (Attewell et al., 1986), may be allowable and is not expected to cause any damage in the buildings. Since subsidence or ground settlement values obtained from both numerical modeling and in situ measurements predict higher settlement values than allowable value, infrastructure in 'risky zone' was investigated and the results were displayed in Fig. 17. Table 10 shows the estimated and observed deformations and subsidence amounts were within compatible ranges.

5.2. Discussion

Underground openings excavated in poor rock formations at shallow depth always bear risks which may eventually influence the structuring on the surface of ground. Considering poor rock quality and tunnel-fault intersection the results obtained from computer models and in situ measurements suggest that enhancement of tunnel support is needed at tunnel-fault transition at the distance (2 + 360 – 2 + 480). Therefore, reduction of the spacing between the rock bolts, use of bored piles, application of umbrella-arch technique, jet-grouting and fiber-grouting may be counted amongst the solutions to minimize the deformations around the opening and consequently to increase the safety of the tunnel.

Bored piles which are often employed with umbrella-arch technique may constrain surface settlements prior to excavation. Nearly 50% of surface settlements in shallow tunnels excavated in poor rock formations usually occur before the tunnel reaches to the measurement station on the surface (Onargan et al., 2006). Owing to the loads applied, the amount of surface settlements may be as much as the amount of the volume of the material which displays plastic behavior and has very low strength. Therefore, an increase in internal parameters of the material on the face of the excavation will be required.

Medium to heavy – heavy support systems will be required at tunnel-fault transition zone where the rock formations possess very low cohesion. The support system projected for both type 1 and type 2 cross sections in this zone presently was the application of shotcrete of 15 cm thickness, steel arches, wire mesh and rock bolts (0.75 × 0.75 m). The results obtained from numerical models and surface settlement measurements clearly suggest that projected support system be insufficient and application of a different support system needs to be proposed for tunnel-fault transition zone, as shown in Fig. 18.

In the proposed support system, application of shotcrete of 5 and 30 cm in thickness at the face and the walls of tunnel respectively (28 day strength value of 21 MPa), two layers of steel wire mesh (Q221/221), rock bolts to be integrated in umbrella arch

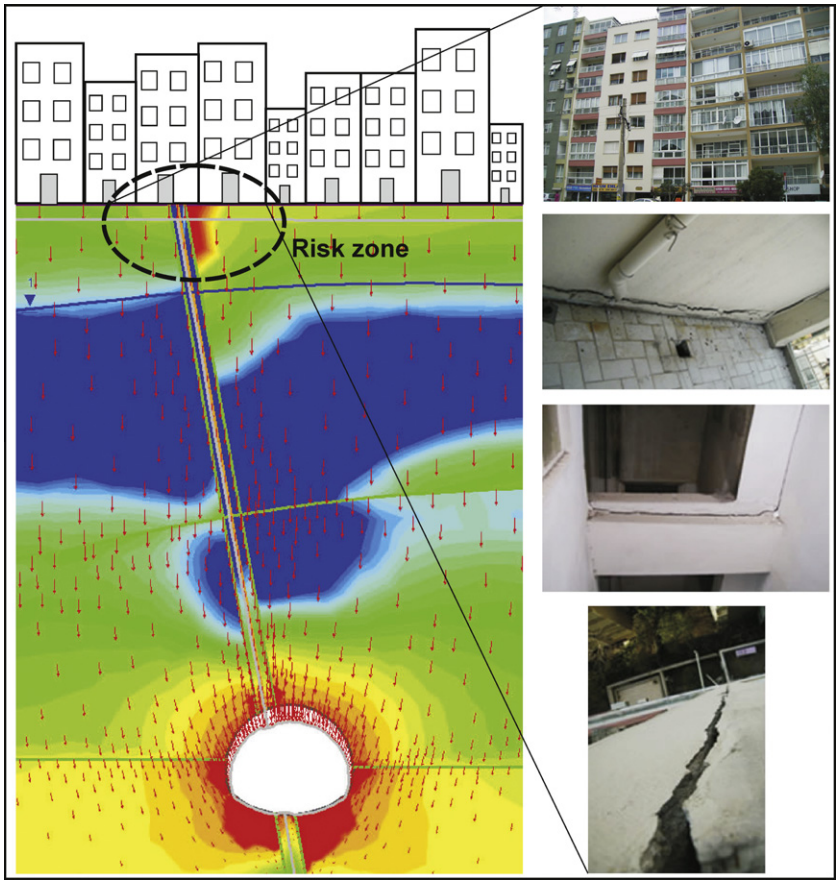

Fig. 17. Damages observed on the ground structures at tunnel-fault zone transition.

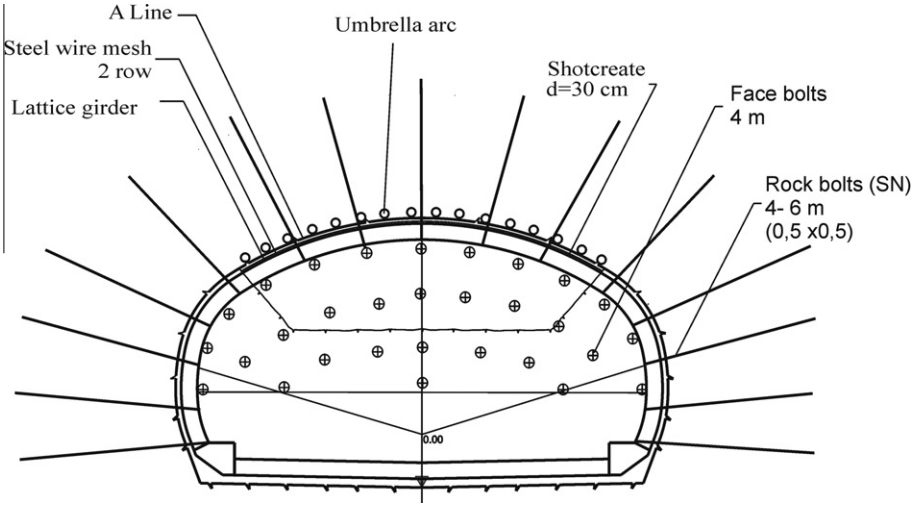

Fig. 18. Proposed support system on fault zone.

technique in a pattern of 0.5 × 0.5 and at bolt spacing of 4–6 m is essential. Length of the steelpipes which will be used in umbrella-arch technique is 4–6 m with an overthrusting amount of 30 cm. If needed, additional techniques such as jet-grouting and injection grouting may be introduced to enhance the tunnel safety.

6. Conclusion

Excavation of an underground tunnel or any opening in rock mass requires evaluation of the geological conditions, determination of rock and soil behavior and analysis of the potential risks in order to complete the structure safely and on time.

Experiences of certain difficulties may be inevitable during the excavation of underground openings in weak rock mass displaying complicated rock–soil properties, which may be also affected by underground water, excavation face stability problems, excessive tunnel and surface deformations. In such conditions, enhancement in projected support system can be suggested both for reducing the damages on the structures situated on the ground surface due to surface settlement resulted from the tunnel deformations and for overall stability/safety of the work.

References

Attewell, P.B., Yeates, J., Selby, A.R., 1986. Soil Movements Induced by Tunneling and their Effects on Pipelines and Structures. Blackie and Son Ltd., London, p. 325.

Barka, A.A., Altunel, E., Akyüz, S., Şaroğlu, F., Emre, Ö., Kuşçu, İ., 1996. Southwestern Slopes of the Anatolian Active Faults and Fault Analysis of Limestone, 1995 Dinar Earthquake and the Tectonic Structure of the Gulf of Saros. TUBITAK National Marine Geology and Geophysics Program. Project Report No.: YDABÇAG-237/G, Ankara, Turkey (in Turkish).

Barton, N., Grimstad, E., 1994. The Q-system following twenty years of application in NMT support selection. Felsbau 12 (6), 428–436.

Bell, F.G., 1994. Engineering in Rock Mass. Butterworths, Great Britain, UK.

Bieniawski, Z.T., 1989. Engineering Rock Mass Classifications. Wiley, New York, USA.

Deere, D.U., Deere, D.W., 1988. In: Kirkaldie, L. (Ed.), The Rock Quality Index in Practice. Rock Classification Systems for Engineering Purposes. ASTM STP 984, pp. 91–101.

Emre, Ö., Barka, A., 2000. Tween the Gediz graben, with the Aegean sea (Izmir region) of active faults. In: Proceedings, Symposium on Seismicity of the Western Anatolia (BADSEM), Izmir, Turkey, pp. 131–132 (in Turkish).

General Directorate of Mineral Research (MTA), 2005. Active Faults and Earthquake Potential of İzmir Surroundings. Project Report No.: 10754. Ankara, Turkey (in Turkish).

ISRM, 1981. In: Brown, E.T. (Ed.), Rock Characterization, Testing and Monitoring, ISRM Suggested Methods. Publ. Pergamon Press, Oxford, p. 211.

Kun, M., 2010. Investigation and Solution of Tunnel Boring Design and Construction Requirements in Weak Rocks and Faulted Zones. Ph.D. Thesis, Dokuz Eylul University, The Graduate School of Natural and Applied Sciences, Izmir, Turkey, p. 220.

Onargan, T., Aksoy, C.O., Güngör, T., Küçük, K., Kun, M., 2006. The Evaluation of Excavation and Support System between Göztepe and F. Altay Stations of 2nd Stage of Izmir Metro Project, Izmir, DEU-MAG, DEUEF, p. 110 (in Turkish).

Onargan, T., Kun, M., Pamukcu, C., Aksoy, C.O., 2009. Development procedure of the New Italian tunnelling method and its application in presupport design at İzmir Metro Bornova tunnel construction. The Journal of The Chamber of Mining Engineers of Turkey 48 (2), 21–34 (in Turkish).

Rocscience Inc., 2006. Phase V6 Software, Canada.

Rocscience Inc., 2006. RocSupport Software, Canada.

Stille, H., Palmstrom, A., 2008. Ground behaviour and rock mass composition in underground excavations. Tunnelling and Underground Space Technology 23, 46–64.

Şaroğlu, F., Emre, Ö., Kuşçu, İ., 1992. Active Fault Map of Turkey. General Directorate of the Mineral Research and Exploration, Ankara, Turkey, 2 Sheets, 1.2000000 Scale (in Turkish).

Ulusay, R., 2001. Geotechnical Applications of Information, vol. 56. TMMOB Chamber of Geological Engineers Publications, Ankara, Turkey, pp. 128–169 (in Turkish).

Whittaker, B.N., Frith, R.C., 1990. Tunneling, Design, Stability and Construction. The Institution of Mining and Metallurgy Press, London, p. 469.